



Cite this: RSC Adv., 2018, 8, 6544

## Effect of OH<sup>-</sup> on chemical mechanical polishing of $\beta$ -Ga<sub>2</sub>O<sub>3</sub> (100) substrate using an alkaline slurry

Chuanjin Huang, <sup>ab</sup> Wenxiang Mu, <sup>c</sup> Hai Zhou, <sup>b</sup> Yongwei Zhu, <sup>\*a</sup> Xiaoming Xu, <sup>b</sup> Zhitai Jia, <sup>c</sup> Lei Zheng <sup>b</sup> and Xutang Tao <sup>\*c</sup>

$\beta$ -Ga<sub>2</sub>O<sub>3</sub>, a semiconductor material, has attracted considerable attention given its potential applications in high-power devices, such as high-performance field-effect transistors. For decades,  $\beta$ -Ga<sub>2</sub>O<sub>3</sub> has been processed through chemical mechanical polishing (CMP). Nevertheless, the understanding of the effect of OH<sup>-</sup> on  $\beta$ -Ga<sub>2</sub>O<sub>3</sub> processed through CMP with an alkaline slurry remains limited. In this study,  $\beta$ -Ga<sub>2</sub>O<sub>3</sub> substrates were successively subjected to mechanical polishing (MP), CMP and etching. Then, to investigate the changes that occurred on the surfaces of the samples, samples were characterised through atomic force microscopy (AFM), three-dimensional laser scanning confocal microscopy (LSCM), scanning electron microscopy (SEM) and X-ray photoelectron spectroscopy (XPS). LSCM and SEM results showed that  $\beta$ -Ga<sub>2</sub>O<sub>3</sub> is highly vulnerable to brittle fracture during MP. AFM revealed that an ultrasmooth and nondamaged surface with a low  $R_a$  of approximately 0.18 nm could be obtained through CMP. XPS results indicated that a metamorphic layer, which mainly contains soluble gallium salt (Ga(OH)<sub>4</sub><sup>-</sup>), formed on the  $\beta$ -Ga<sub>2</sub>O<sub>3</sub> surface through a chemical reaction. A dendritic pattern appeared on the surface of  $\beta$ -Ga<sub>2</sub>O<sub>3</sub> after chemical etching. This phenomenon indicated that the chemical reaction on the  $\beta$ -Ga<sub>2</sub>O<sub>3</sub> surface occurred in a nonuniform and selective manner. The results of this study will aid the optimization of slurry preparation and CMP.

Received 19th October 2017  
Accepted 4th February 2018

DOI: 10.1039/c7ra11570a  
[rsc.li/rsc-advances](http://rsc.li/rsc-advances)

## 1 Introduction

The application of  $\beta$ -type gallium oxide ( $\beta$ -Ga<sub>2</sub>O<sub>3</sub>) as a semiconductor material of high-power devices,<sup>1–3</sup> such as high-performance field-effect transistors,<sup>4,5</sup> Schottky barrier diodes<sup>6,7</sup> and ultraviolet transparent electrodes,<sup>8</sup> has attracted considerable attention because  $\beta$ -Ga<sub>2</sub>O<sub>3</sub> has excellent material properties, including a wide band gap of approximately 4.9 eV, and stable chemical and thermal properties.<sup>9</sup> Although numerous studies have been conducted on  $\beta$ -Ga<sub>2</sub>O<sub>3</sub> materials,<sup>10–14</sup> few have focused on the ultraprecision machining of these materials. Chemical mechanical polishing (CMP), a key step in the ultraprecision machining of crystal materials, is an efficient technique that yields ultrasmooth and undamaged crystal surfaces.<sup>15</sup>

The main cleavage plane of the  $\beta$ -Ga<sub>2</sub>O<sub>3</sub> crystal is along its (100) surface,<sup>16</sup> which is the most thermodynamically stable and the most suitable surface for thin-film growth among all surfaces.<sup>17</sup> However, cleavage renders the crystal surface fragile

and hinders the ultraprecise machining of  $\beta$ -Ga<sub>2</sub>O<sub>3</sub>.<sup>2</sup> Ga–O bonds in the unstable octahedral of the  $\beta$ -Ga<sub>2</sub>O<sub>3</sub> (100) structure fracture easily.<sup>16</sup> The  $\beta$ -Ga<sub>2</sub>O<sub>3</sub> (100) structure is composed of a slightly distorted tetrahedral and a highly distorted octahedral. Ga–O bonds in  $\beta$ -Ga<sub>2</sub>O<sub>3</sub> (100) are highly sensitive to mechanical stress and cause crystal cleavage during processing. Therefore, chemical action may be a feasible method for generating new bonds that can shield Ga–O bonds during CMP.<sup>18–20</sup> Slurries with alkali and oxidisers applied in the CMP of GaN and GaAs can be applied in the CMP of  $\beta$ -Ga<sub>2</sub>O<sub>3</sub>.<sup>18,20,21</sup> However, gallium oxide is in a stable oxidation state, and wet etching experiments on  $\beta$ -Ga<sub>2</sub>O<sub>3</sub> are utilised only as a reference for evaluating the use of sodium hydroxide as a mordant without an oxidant.<sup>22,23</sup> The  $\beta$ -Ga<sub>2</sub>O<sub>3</sub> (100) surface needs to be processed through CMP using an alkaline slurry with OH<sup>-</sup> to obtain an ultrasmooth crystal surface. Moreover, the chemical action mechanism that underlies the CMP of  $\beta$ -Ga<sub>2</sub>O<sub>3</sub> must be investigated.

By evaluating the morphology and chemical composition of the  $\beta$ -Ga<sub>2</sub>O<sub>3</sub> surface after treatment, this study investigated the effect of OH<sup>-</sup> on  $\beta$ -Ga<sub>2</sub>O<sub>3</sub> processed through mechanical polishing (MP) without chemical action and to CMP with chemical action. Moreover, the chemical action between  $\beta$ -Ga<sub>2</sub>O<sub>3</sub> and sodium hydroxide during wet etching was investigated. The surface morphology of  $\beta$ -Ga<sub>2</sub>O<sub>3</sub> was examined through atomic force microscopy (AFM), laser-scanning confocal microscopy

<sup>a</sup>College of Mechanical and Electrical Engineering, Nanjing University of Aeronautics and Astronautics, Nanjing 210016, China. E-mail: [meeywzhu@nuaa.edu.cn](mailto:meeywzhu@nuaa.edu.cn)

<sup>b</sup>College of Mechanical Engineering, Yancheng Institute of Technology, Yancheng 224051, China

<sup>c</sup>State Key Laboratory of Crystal Materials, Key Laboratory of Functional Crystal Materials and Device, Shandong University, Jinan, 250100, China. E-mail: [txt@sdu.edu.cn](mailto:txt@sdu.edu.cn)



(LSCM) and scanning electron microscopy (SEM). Results indicated that a metamorphic layer that formed on the crystal surface through a chemical reaction was removed during CMP. X-ray photoelectron spectroscopy (XPS) was also used to study the surface chemistry of  $\beta$ -Ga<sub>2</sub>O<sub>3</sub>. The different chemical states of the metamorphic layer during different treatment processes were studied. This experimental analysis may be useful for optimising slurry preparation.

## 2 Material and methods

$\beta$ -Ga<sub>2</sub>O<sub>3</sub> substrates were cut from a crystal bar along the (100) plane and prepared *via* the edge-defined film-fed crystal growth method. The  $\beta$ -Ga<sub>2</sub>O<sub>3</sub> (100) substrates had a size of approximately 10 mm  $\times$  10 mm  $\times$  1 mm (length  $\times$  width  $\times$  thickness). Prior to the experiments, the substrates were ground to expose a large flat surface, which served as the foundation of subsequent experiments.

This experiment comprised three steps, as follows: firstly, the substrates were treated through MP.  $\beta$ -Ga<sub>2</sub>O<sub>3</sub> was polished using a polishing tester (UNIPOL-1502, MTI-KJ Corp., Ltd.) with silk as a soft pad at a pressure of 15 kPa. Deionised water (DI) and diamond paste (mean diameter 1  $\mu$ m) were used as chemically inert lapping media. The other process conditions were as follows: plate speed of 35 rpm and polishing time of 4 h. Secondly, the substrates were treated through CMP.  $\beta$ -Ga<sub>2</sub>O<sub>3</sub> was polished with the same polishing tester equipped with an Politex pad (Rohm & Haas Co., Ltd.). Commercial colloidal silica (NS-54, Fuso Chemical Co., Ltd.) mixed with diluted sodium hydroxide was used as the slurry. Slurry pH was adjusted to 11, and slurry concentration was approximately 20 wt%. The slurry was not reused. The other process conditions were as follows: plate rotation speed of 35 rpm, operating pressure of 15 kPa, slurry flow rate of 50 mL min<sup>-1</sup> and polishing time of 15 h. Finally, the  $\beta$ -Ga<sub>2</sub>O<sub>3</sub> substrates were etched with 20 wt% sodium hydroxide solution at 55 °C for 2 h. The substrates were successively cleaned with liquid cleaner, DI water and ethyl alcohol and dried by an air spray gun for each measurement.

The surface morphology of  $\beta$ -Ga<sub>2</sub>O<sub>3</sub> after treatment was characterised using Keyence VK-X110K 3D LSCM, FEI Nova NanoSEM 450 and Bruker Dimension Icon AFM. The surface average roughness ( $R_a$ ) values after MP were determined using

LSCM with 100  $\mu$ m  $\times$  100  $\mu$ m scans.  $R_a$  after CMP was determined through AFM with 1  $\mu$ m  $\times$  1  $\mu$ m scans. The surface chemical composition was analysed with Thermo Scientific Escalab250Xi (XPS). Firstly, samples subjected to MP, CMP and etching were studied. The surfaces of these samples were measured in normal mode with 0° electron emission angle. Secondly, to analyse the chemical composition of the crystal surface subjected to CMP, the crystal surface was measured in angle-resolved mode with an electron emission angle of 0° to 75°. All data were obtained using a monochromatised Al-K $\alpha$  source (1486.6 eV) and a pass energy of 40 eV. XPS peak assignment was based on an acceptable standard reference database and literature reports.<sup>17,24-26</sup>

## 3 Results and discussion

### 3.1 Surface morphology analysis

The AFM images of the CMP-treated  $\beta$ -Ga<sub>2</sub>O<sub>3</sub> surface are shown in Fig. 1. The  $R_a$  of the sample was approximately 0.18 nm. The surface did not exhibit a regular terraced morphology but instead exhibited negligible roughness similar to that reported in previous studies.<sup>27,28</sup> This result indicated that the wafer surface might have been covered with a layer of chemical substances. The ultrasmooth surface of the wafer processed through CMP is shown in Fig. 1. The wafer exhibited surface contamination, which is shown as a series of brightly coloured points.<sup>29</sup> The properties of the polished surface with residual chemical products were characterised through SEM and XPS to identify the chemical action mechanism that underlies the CMP of  $\beta$ -Ga<sub>2</sub>O<sub>3</sub>.

The surface morphology of  $\beta$ -Ga<sub>2</sub>O<sub>3</sub> treated through MP, CMP and etching are shown in Fig. 2. As shown in Fig. 2(a) and (d), after MP treatment, the substrate appeared rough with an  $R_a$  of 52 nm and was covered with tongue-patterned cleavage pits. During MP, abrasive diamond grains cut into the crystal plane and resulted in the instantaneous generation of concentrated stress. New cracks were initiated on the crystal plane, and crack expansion accelerated until the plane underwent low-energy brittle fracture, which is very easy to occur because of the cleavage of  $\beta$ -Ga<sub>2</sub>O<sub>3</sub>. After CMP, the surface  $R_a$  of the  $\beta$ -Ga<sub>2</sub>O<sub>3</sub> substrate decreased from 54 nm to 0.18 nm, and the cleavage pits disappeared. The ultrasmooth mirror-like surface of the

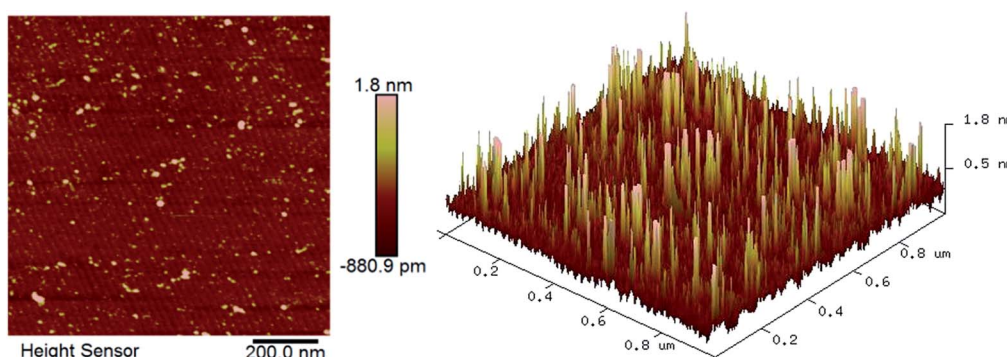


Fig. 1 AFM images of  $\beta$ -Ga<sub>2</sub>O<sub>3</sub> after CMP.



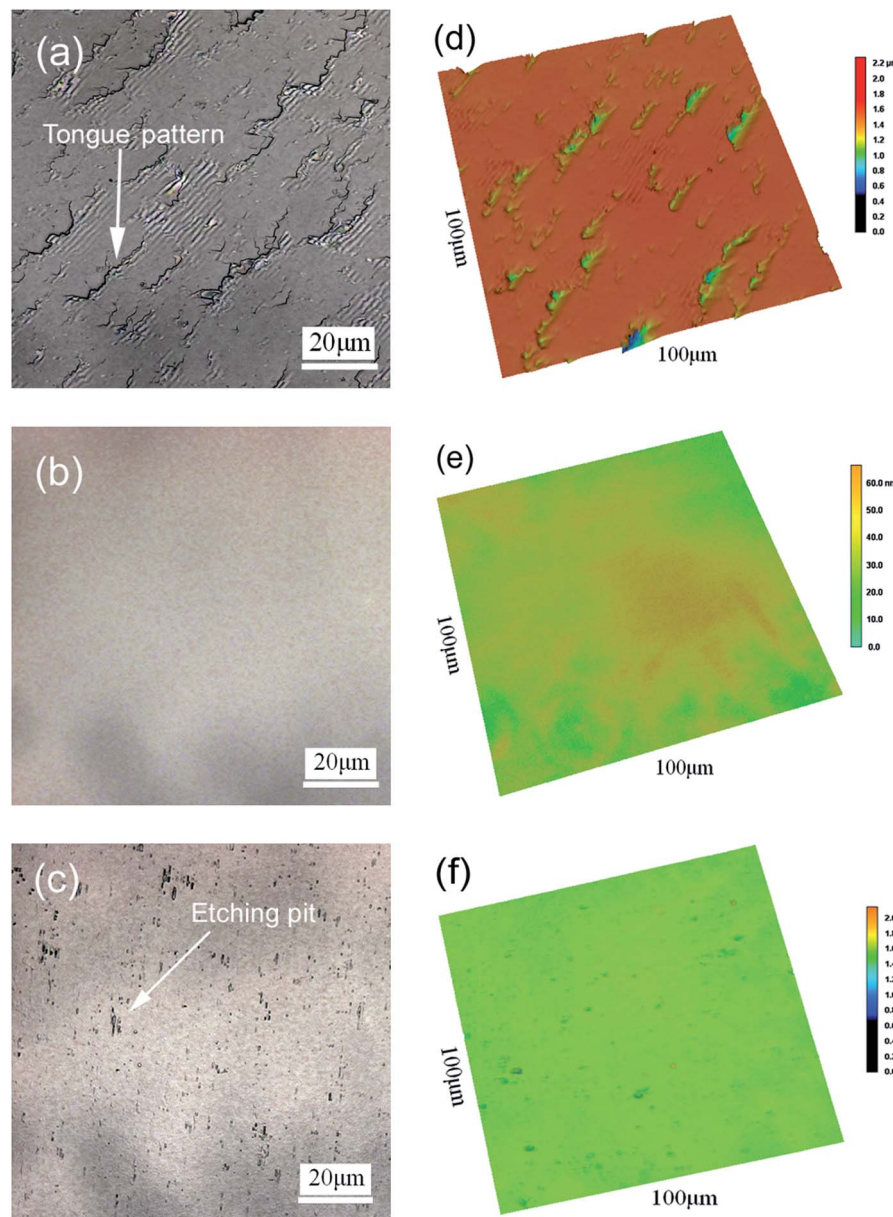


Fig. 2 Two-dimensional LSCM images of  $\beta$ - $\text{Ga}_2\text{O}_3$  (100) after (a) MP, (b) CMP and (c) etching. (d), (e) and (f) are the corresponding three-dimensional images of (a), (b) and (c).

substrate obtained after CMP is shown in Fig. 2(b) and (e). Micro cleavage pits caused by local cleavage fracture were difficult to remove during MP, as shown in Fig. 2(a) and (b). By contrast, micro cleavage pits were easily removed during CMP because  $\beta$ - $\text{Ga}_2\text{O}_3$  was chemically corroded in the alkaline environment. Numerous etching pits were present on the surface of  $\beta$ - $\text{Ga}_2\text{O}_3$ , as shown in Fig. 2(c) and (f). This pattern indicated that a chemical reaction occurred between  $\text{Ga}_2\text{O}_3$  and sodium hydroxide. The surface morphology of the  $\beta$ - $\text{Ga}_2\text{O}_3$  substrate dramatically changed through chemical action.

The crystal surfaces obtained through different processes using slurries containing sodium hydroxide were subjected to microscopy observation to describe the chemical mechanism that acts on  $\beta$ - $\text{Ga}_2\text{O}_3$  during CMP. The SEM images of the

surfaces treated through MP, CMP and etching are shown in Fig. 3. As shown in Fig. 3(a), numerous scratches formed on the crystal surface after MP. Scratches between cleavage pits appeared flat, as shown in Fig. 2(a). The crisscrossing micro-scratches indicated that the cleavage properties of  $\beta$ - $\text{Ga}_2\text{O}_3$  caused microscratch defects even when abrasive grains did not produce cleavage pits after the crystal face was cut. An ultra-smooth mirror-like surface was obtained after CMP, as shown in Fig. 3(b). This surface exhibited fewer cleavage defects than the surface shown in Fig. 3(a). Fig. 3(c) shows the  $\beta$ - $\text{Ga}_2\text{O}_3$  surface after etching with sodium hydroxide solution and CMP. The crystal face exhibited a dendritic pattern. The bright section of the dendritic pattern shown in Fig. 3(c) represented a protruding structure similar to a peak, and the remaining grey



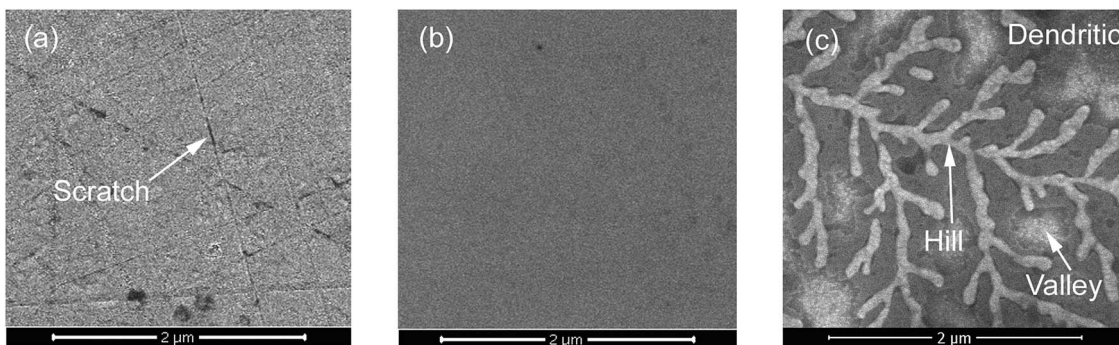


Fig. 3 SEM images of the  $\beta$ - $\text{Ga}_2\text{O}_3$  surface after (a) MP, (b) CMP and (c) etching.

portion indicated a low-lying area similar to a valley. The presence of dendrites implied that sodium hydroxide selectively corrodes  $\beta$ - $\text{Ga}_2\text{O}_3$ . The valleys of the crystal surface indicated areas that are susceptible to corrosion under alkaline conditions, and the peaks indicated areas that are relatively resistant to corrosion. Generally,  $\beta$ - $\text{Ga}_2\text{O}_3$  exhibits uneven corrosion under alkaline conditions during CMP. Therefore, the use of abrasive silica particles to remove the residual metamorphic layer is an essential step in CMP.

The formation and removal of the metamorphic layer on the surface of  $\beta$ - $\text{Ga}_2\text{O}_3$  during CMP are important for obtaining an ultrasmooth surface. The chemical composition of the metamorphic layer was analysed.

### 3.2 Surface chemical composition analysis

As shown in Fig. 4, peaks that correspond to Ga 3d, O 1s and C 1s photoelectrons are present in the survey scan spectra of the  $\beta$ - $\text{Ga}_2\text{O}_3$  substrates treated through MP, CMP and etching. The prominent C 1s peaks observed in all wide-survey XPS spectra may have originated from the adsorption of adventitious carbon contaminants on the surface; these contaminants could be partly removed by heat treatment.<sup>17</sup> The C 1s peak at 284.8 eV could be used to calibrate the peak positions of other elements. Fig. 4 also shows that surface contaminants can be attributed to different processes. For example, Fe was contributed by the iron plate during grinding, and Na was contributed by the slurry used for CMP. These contaminants could be removed through

subsequent processes. The spectra of the surfaces would be similar if the effect of Fe and Na contaminants are ignored.

Fig. 5 shows the Ga 3d and O 1s XPS spectra of the  $\beta$ - $\text{Ga}_2\text{O}_3$  surface after various treatments. Curve fitting was performed by using the Shirley background, and the symmetric Lorentzian–Gaussian peak shape function value was set as 20%. The evolution of the Ga 3d XPS spectra of the  $\beta$ - $\text{Ga}_2\text{O}_3$  surface after different treatments is illustrated in Fig. 5(a)–(c). Fig. 5(a) shows that the peak representing the Ga–O bond of  $\beta$ - $\text{Ga}_2\text{O}_3$  is located at 20.4 eV after MP, whereas that representing O 2s, which could be attributed to the hybridization of the Ga 3d and O 2s surface states, is located at 24 eV.<sup>24</sup> Fig. 5(a)–5(b) show that the Ga 3d peak acquired at normal emission shifted to a low binding energy from MP to CMP. This shift was caused by a chemical reaction. After CMP, the peak position shifted by approximately 0.9 eV from 20.4 eV (Ga–O bond) to 19.5 eV (Ga–OH bond).<sup>26</sup> This shift could be attributed to the breakage of Ga–O bonds through a tribochemical action, which allowed surface Ga to bond with hydroxyl from sodium hydroxide. This result suggested that the surface of  $\beta$ - $\text{Ga}_2\text{O}_3$  undergoes tribochemical reactions with sodium hydroxide to form new reaction products, such as soluble gallium salt ( $\text{Ga}(\text{OH})_4^-$ ), during CMP.<sup>18</sup> These salts were then partly absorbed on the polished surface. Chemical reactions during CMP and etching exhibited similar results, as shown in Fig. 5(c). A detailed analysis of the O 1s core level peaks of the substrate is shown in Fig. 5(d)–(f). The O 1s peaks at 531.4, 532.8 and 530.9 eV observed after MP and shown in Fig. 5(d) could be respectively attributed to the main Ga–O bond peak,<sup>24</sup> C–O from carbon contaminants<sup>17</sup> and Fe–O contributed by cast-iron grinding discs before MP.<sup>26</sup> Fig. 5(d)–(f) show that the Ga–O bond of  $\beta$ - $\text{Ga}_2\text{O}_3$  was replaced by Ga–OH after CMP and etching due to chemical action, indicating that the same condition shown by Fig. 5(a)–(c) was observed for CMP. Moreover, the low full width at half maximum (FWHM) of the Ga 3d and O 1s peaks observed from Fig. 5(b) and (e) indicated the excellent crystalline quality of the studied samples.<sup>9</sup>

Fig. 6 shows the variation tendency of the atomic composition, including Ga, O, C and Na, of the  $\beta$ - $\text{Ga}_2\text{O}_3$  surface layer after CMP. The atomic composition of the  $\beta$ - $\text{Ga}_2\text{O}_3$  surface layer was identified through angle-resolved XPS (ARXPS). The Ga-to-O ratio of the  $\beta$ - $\text{Ga}_2\text{O}_3$  surface layer significantly increased with surface depth and was close to the stoichiometric ratio of 2/3,

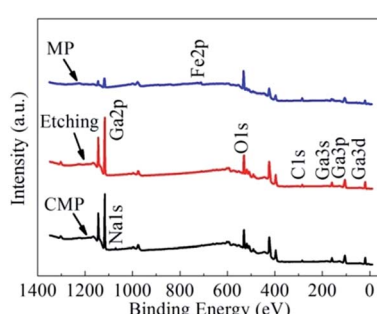


Fig. 4 Wide-survey XPS spectra of  $\beta$ - $\text{Ga}_2\text{O}_3$  after CMP, etching and MP.



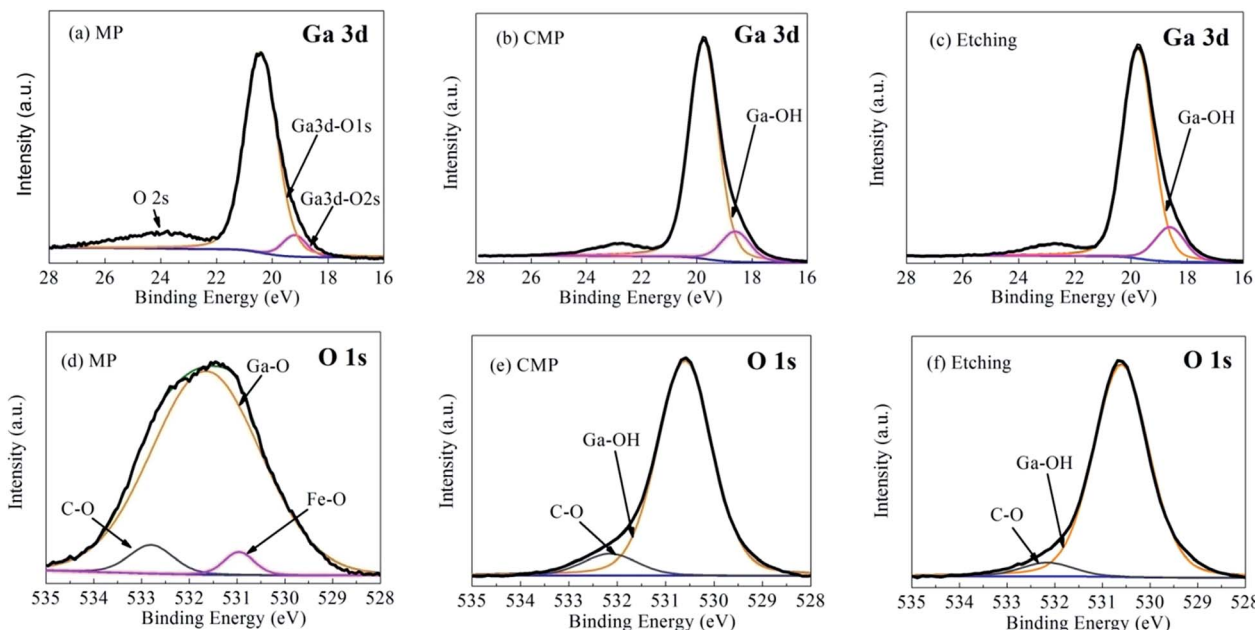


Fig. 5 (a)–(f) Fitted Ga 3d and O 1s XPS spectra of  $\beta$ -Ga<sub>2</sub>O<sub>3</sub> after MP, CMP and etching.

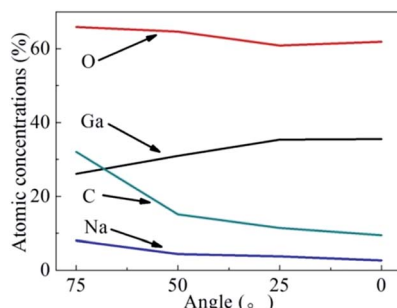


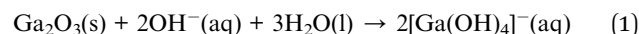
Fig. 6 ARXPS results of the  $\beta$ -Ga<sub>2</sub>O<sub>3</sub> surface layer treated through CMP.

indicating that gallium salts and other oxide contaminants may be distributed on the surface. Trace amounts of metal contaminants, such as Na, were present on the surface and were likely contributed by the slurry containing sodium hydroxide. Fig. 4 and 6 suggested that metal ions can penetrate the crystal surface through mechanical abrasion during CMP but not during static etching. To prevent metal pollution, the slurry formula must be optimised by selecting the appropriate organic alkali and a suitable complexing agent.<sup>19,29–31</sup> An extremely thin metamorphic layer was adsorbed on the crystal surface treated through CMP. This layer is useful for removing surface crystal materials during CMP.

### 3.3 Polishing mechanisms

The chemical action mechanism of  $\beta$ -Ga<sub>2</sub>O<sub>3</sub> is summarised as the formation of a metamorphic surface layer. Firstly, XPS data shown in Fig. 5 indicated that the chemical action mechanism underlying CMP can be used to describe the formation of the

metamorphic layer. When Ga<sub>2</sub>O<sub>3</sub> was subjected to CMP with alkali hydroxide under basic pH, reaction products that contain gallium salts, such as Ga(OH)<sub>4</sub><sup>–</sup>, may leave a film on the crystal surface.<sup>20</sup> The reaction that yields gallium salt is as follows:



SEM data shown in Fig. 3 revealed that a dendritic pattern appeared on the  $\beta$ -Ga<sub>2</sub>O<sub>3</sub> crystal surface after immersion in slurry containing sodium hydroxide. This pattern indicated that the surface corrosion of  $\beta$ -Ga<sub>2</sub>O<sub>3</sub> is selective and that generation of new metamorphic layers is uneven. Rugged metamorphic layers could be uniformly removed through mechanical abrasion to yield ultrasmooth, nondamaged crystal surfaces.

A metamorphic layer formed on the surface of  $\beta$ -Ga<sub>2</sub>O<sub>3</sub> through a chemical reaction during CMP under alkaline conditions. This layer was mainly composed of gallium salts. The adsorption of these salts on the  $\beta$ -Ga<sub>2</sub>O<sub>3</sub> surface changed the physical and chemical properties of the crystal surface, such as hardness, brittleness, wettability and hydrolysability, thus improving the processing properties of the crystal. Therefore, the generation of a metamorphic layer influences material removal during CMP and mitigates cleavage during polishing.

## 4 Conclusions

$\beta$ -Ga<sub>2</sub>O<sub>3</sub> (100) surfaces were treated through MP, CMP and etching. The treated surfaces were then characterised through AFM, LSCM, SEM and XPS to reveal the effect of sodium hydroxide on ultraprecision polishing. The LSCM results showed that the cleavage of  $\beta$ -Ga<sub>2</sub>O<sub>3</sub> hindered the processing of crystals to an ultrasmooth surface, and the apparent fragility of the crystal during MP resulted in the formation of surface



micropits. SEM and XPS results proved that the formation of a metamorphic layer on the surface of  $\beta$ -Ga<sub>2</sub>O<sub>3</sub> has a critical role in the removal of materials formed by the chemical reaction between Ga<sub>2</sub>O<sub>3</sub> and sodium hydroxide during CMP. Ga-O bonds on the surface of  $\beta$ -Ga<sub>2</sub>O<sub>3</sub> replaced cleaved Ga-OH bonds, leading to the formation of soluble gallium salts. The metamorphic layer can be easily removed during CMP to prevent surface damage. SEM results showed that dendritic patterns formed on the crystal surface after etching. These patterns indicated that  $\beta$ -Ga<sub>2</sub>O<sub>3</sub> is nonuniformly and selectively corroded during chemical reaction due to. AFM indicated that an ultrasmooth surface with a low  $R_a$  of approximately 0.18 nm was obtained through CMP. In summary, the chemical reaction of OH<sup>-</sup> on  $\beta$ -Ga<sub>2</sub>O<sub>3</sub> may help aid the optimisation of slurry preparation for CMP.

## Conflicts of interest

There are no conflicts to declare.

## Acknowledgements

This work has been supported by The National Natural Science Foundation of China (No. 51675457 and 51575470), Joint Innovation Fund Project of Jiangsu Province (BY2016065-55).

## References

- 1 M. Higashiwaki, K. Sasaki, A. Kuramata, T. Masui and S. Yamakoshi, Development of gallium oxide power devices, *Phys. Status Solidi A*, 2014, **211**, 21–26.
- 2 E. G. Víllora, S. Arjoca, K. Shimamura, D. Inomata and K. Aoki,  $\beta$ -Ga<sub>2</sub>O<sub>3</sub> and single-crystal phosphors for high-brightness white LEDs and LDs, and  $\beta$ -Ga<sub>2</sub>O<sub>3</sub> potential for next generation of power devices, *Proc. SPIE-Int. Soc. Opt. Eng.*, 2014, 89871U.
- 3 W. Mu, Y. Yin, Z. Jia, L. Wang, J. Sun, M. Wang, C. Tang, Q. Hu, Z. Gao, J. Zhang, N. Lin, S. Veronesi, Z. Wang, X. Zhao and X. Tao, An extended application of  $\beta$ -Ga<sub>2</sub>O<sub>3</sub> single crystals to the laser field: Cr<sup>4+</sup>: $\beta$ -Ga<sub>2</sub>O<sub>3</sub> utilized as a new promising saturable absorber, *RSC Adv.*, 2017, **7**, 21815–21819.
- 4 M. Higashiwaki, K. Sasaki, T. Kamimura, M. Hoi Wong, D. Krishnamurthy, A. Kuramata, T. Masui and S. Yamakoshi, Depletion-mode Ga<sub>2</sub>O<sub>3</sub> metal-oxide-semiconductor field-effect transistors on  $\beta$ -Ga<sub>2</sub>O<sub>3</sub> (010) substrates and temperature dependence of their device characteristics, *Appl. Phys. Lett.*, 2013, **103**, 123511.
- 5 M. Higashiwaki, K. Sasaki, A. Kuramata, T. Masui and S. Yamakoshi, Gallium oxide (Ga<sub>2</sub>O<sub>3</sub>) metal-semiconductor field-effect transistors on single-crystal  $\beta$ -Ga<sub>2</sub>O<sub>3</sub> (010) substrates, *Appl. Phys. Lett.*, 2012, **100**, 013504.
- 6 R. Suzuki, S. Nakagomi, Y. Kokubun, N. Arai and S. Ohira, Enhancement of responsivity in solar-blind  $\beta$ -Ga<sub>2</sub>O<sub>3</sub> photodiodes with a Au Schottky contact fabricated on single crystal substrates by annealing, *Appl. Phys. Lett.*, 2009, **94**, 222102.
- 7 M. Higashiwaki, K. Konishi, K. Sasaki, K. Goto, K. Nomura, Q. T. Thieu, R. Togashi, H. Murakami, Y. Kumagai and M. Bo, Temperature-dependent capacitance-voltage and current-voltage characteristics of Pt/Ga<sub>2</sub>O<sub>3</sub> (001) Schottky barrier diodes fabricated on  $n$ -Ga<sub>2</sub>O<sub>3</sub> drift layers grown by halide vapor phase epitaxy, *Appl. Phys. Lett.*, 2016, **108**, 1759.
- 8 M. Zhong, Z. Wei, X. Meng, F. Wu and J. Li, High-performance single crystalline UV photodetectors of  $\beta$ -Ga<sub>2</sub>O<sub>3</sub>, *J. Alloys Compd.*, 2015, **619**, 572–575.
- 9 W. Mu, Z. Jia, Y. Yin, Q. Hu, Y. Li, B. Wu, J. Zhang and X. Tao, High quality crystal growth and anisotropic physical characterization of  $\beta$ -Ga<sub>2</sub>O<sub>3</sub> single crystals grown by EFG method, *J. Alloys Compd.*, 2017, **714**, 453–458.
- 10 Y. Liu and Z. H. Li, Adsorption and decomposition mechanism of formic acid on the Ga<sub>2</sub>O<sub>3</sub> surface by first principle studies, *Surf. Sci.*, 2017, **656**, 86–95.
- 11 H. Yamaguchi, A. Kuramata and T. Masui, Slip system analysis and X-ray topographic study on  $\beta$ -Ga<sub>2</sub>O<sub>3</sub>, *Superlattices Microstruct.*, 2016, 99.
- 12 K. Hanada, T. Moribayashi, T. Uematsu, S. Masuya, K. Koshi, K. Sasaki, A. Kuramata, O. Ueda and M. Kasu, Observation of nanometer-sized crystalline grooves in as-grown  $\beta$ -Ga<sub>2</sub>O<sub>3</sub> single crystals, *Jpn. J. Appl. Phys.*, 2016, **55**, 030303.
- 13 L. Feng, Y. Li, X. Su, S. Wang, H. Liu, J. Wang, Z. Gong, W. Ding, Y. Zhang and F. Yun, Growth and characterization of spindle-like Ga<sub>2</sub>O<sub>3</sub> nanocrystals by electrochemical reaction in hydrofluoric solution, *Appl. Surf. Sci.*, 2016, **389**, 205–210.
- 14 T. Onuma, S. Fujioka, T. Yamaguchi, Y. Itoh, M. Higashiwaki, K. Sasaki, T. Masui and T. Honda, Polarized Raman spectra in  $\beta$ -Ga<sub>2</sub>O<sub>3</sub> single crystals, *J. Cryst. Growth*, 2014, **401**, 330–333.
- 15 Y. Chen, A. Chen and J. Qin, Polystyrene core–silica shell composite particles: effect of mesoporous shell structures on oxide CMP and mechanical stability[J], *RSC Adv.*, 2017, **7**(11), 6548–6558.
- 16 V. M. Bermudez, The structure of low-index surfaces of  $\beta$ -Ga<sub>2</sub>O<sub>3</sub>, *Chem. Phys.*, 2006, **323**, 193–203.
- 17 A. Navarro-Quezada, Z. Galazka, S. Alamé, D. Skuridina, P. Vogt and N. Esser, Surface properties of annealed semiconducting  $\beta$ -Ga<sub>2</sub>O<sub>3</sub> (100) single crystals for epitaxy, *Appl. Surf. Sci.*, 2015, **349**, 368–373.
- 18 J. B. Matovu, P. Ong, L. H. A. Leunissen, S. Krishnan and S. V. Babu, Fundamental Investigation of Chemical Mechanical Polishing of GaAs in Silica Dispersions: Material Removal and Arsenic Trihydride Formation Pathways, *ECS J. Solid State Sci. Technol.*, 2013, **2**, 432–439.
- 19 R. R. Nair, A. Gupta, S. N. Victoria and R. Manivannan, Chemical mechanical planarization of germanium using oxone® based silica slurries, *Wear*, 2017, **376–377**, 86–90.
- 20 J. Wang, T. Wang, G. Pan and X. Lu, Effect of photocatalytic oxidation technology on GaN CMP, *Appl. Surf. Sci.*, 2016, **361**, 18–24.
- 21 H. Aida, T. Doi, H. Takeda, H. Kataura, S. W. Kim, K. Koyama, T. Yamazaki and M. Uneda, Ultraprecision CMP for sapphire, GaN, and SiC for advanced optoelectronics materials, *Curr. Appl. Phys.*, 2012, **12**, S41–S46.



22 S. Ohira and N. Arai, Wet chemical etching behavior of  $\beta$ - $\text{Ga}_2\text{O}_3$  single crystal, *Phys. Status Solidi C*, 2008, **5**, 3116–3118.

23 T. Oshima, T. Okuno, N. Arai, Y. Kobayashi and S. Fujita, Wet Etching of  $\beta$ - $\text{Ga}_2\text{O}_3$  Substrates, *Jpn. J. Appl. Phys.*, 2009, **48**, 040208.

24 A. Navarro-Quezada, S. Alamé, N. Esser, J. Furthmüller, F. Bechstedt, Z. Galazka, D. Skuridina and P. Vogt, Near valence-band electronic properties of semiconducting  $\beta$ - $\text{Ga}_2\text{O}_3$  (100) single crystals, *Phys. Rev. B*, 2015, **92**, 195306.

25 A. I. Serykh and M. D. Amiridis, *In situ* X-ray photoelectron spectroscopy study of supported gallium oxide, *Surf. Sci.*, 2010, **604**, 1002–1005.

26 NIST X-ray Photoelectron Spectroscopy Database, <https://srdata.nist.gov/xps/>.

27 X. Shi, C. Zou, G. Pan, H. Gong, L. Xu and Y. Zhou, Atomically smooth gallium nitride surface prepared by chemical-mechanical polishing with  $\text{S}_2\text{O}_8^{2-}$ – $\text{Fe}^{2+}$  based slurry, *Tribol. Int.*, 2017, **110**, 441–450.

28 Y. Zhou, G. Pan, H. Gong, X. Shi and C. Zou, Characterization of sapphire chemical mechanical polishing performances using silica with different sizes and their removal mechanisms, *Colloids Surf., A*, 2017, **513**, 153–159.

29 X. Shi, G. Pan, Y. Zhou, L. Xu, C. Zou and H. Gong, A study of chemical products formed on sapphire (0001) during chemical-mechanical polishing, *Surf. Coat. Technol.*, 2015, **270**, 206–220.

30 K. Yadav, J. C. Bisen, S. N. Victoria and R. Manivannan, Sodium hypochlorite as an oxidizing agent in silica based ruthenium chemical mechanical planarization slurry, *Microelectron. Eng.*, 2017, **180**, 96–100.

31 K. Asghar, M. Qasim, D. M. Nelabhotla and D. Das, Effect of surfactant and electrolyte on surface modification of c-plane GaN substrate using chemical mechanical planarization (CMP) process, *Colloids Surf., A*, 2016, **497**, 133–145.

